

Photoemission spectrum and effect of inhomogeneous pairing fluctuations in the BCS-BEC crossover regime of an ultracold Fermi gas

Shunji Tsuchiya,^{1,2} Ryota Watanabe,¹ and Yoji Ohashi^{1,2}

¹*Department of Physics, Keio University, 3-14-1 Hiyoshi, Kohoku-ku, Yokohama 223-8522, Japan*

²*CREST(JST), 4-1-8 Honcho, Saitama 332-0012, Japan*

(Dated: February 14, 2022)

We investigate the photoemission-type spectrum in a cold Fermi gas which was recently measured by JILA group [J. T. Stewart *et al.*, *Nature* **454**, 744 (2008)]. This quantity gives us very useful information about single-particle properties in the BCS-BEC crossover. In this letter, including pairing fluctuations within a T -matrix theory, as well as effects of a harmonic trap within the local density approximation, we show that spatially inhomogeneous pairing fluctuations due to the trap potential is an important key to understand the observed spectrum. In the crossover region, while strong pairing fluctuations lead to the so-called pseudogap phenomenon in the trap center, such strong-coupling effects are found to be weak around the edge of the gas. Our results including this effect are shown to agree well with the recent photoemission data by JILA group.

PACS numbers: 03.75.Ss, 05.30.Fk, 67.85.-d

The recent photoemission-type experiment developed by JILA group[1] provides a powerful method to study microscopic properties of cold Fermi gases. This experiment is an analogue of angle-resolved photoemission spectroscopy (ARPES)[2], which has been extensively applied in condensed matter physics. Using this technique, one can probe single-particle excitations that allow us to investigate many-body effects in the BCS-BEC crossover[3–14]. Indeed, the observed spectra exhibit dramatic change in the crossover region[1].

One typical many-body effect on single-particle excitations expected in the BCS-BEC crossover regime of a cold Fermi gas is the pseudogap effect. In this phenomenon, preformed pairs cause a gap-like structure in the density of states (DOS) even above the superfluid phase transition temperature T_c . The pseudogap has been observed in the underdoped regime of high- T_c cuprates[15]. However, as the origin of this phenomenon in high- T_c cuprates, in addition to pairing fluctuations, various possibilities have been proposed, such as spin fluctuations and a hidden order. Since the BCS-BEC crossover in a cold Fermi gas is dominated by pairing fluctuations, the study of pseudogap in this system would be also useful for clarifying the validity of the pseudogap mechanism based on preformed pairs in high- T_c cuprates. Since the pseudogap appears in single-particle excitations, the photoemission experiment would be useful for this purpose.

In considering the pseudogap effect in cold Fermi gases, one should note that the presence of a trap naturally leads to spatially inhomogeneous pairing fluctuations. While the pseudogap structure in DOS is expected to be remarkable in the trap center, such a many-body effect may be weak around the edge of gas cloud. Since the pseudogap in high- T_c cuprates is a uniform phenomenon, this inhomogeneous pseudogap effect is unique to trapped Fermi gases. Indeed, the double-peak structure in the photoemission spectrum observed in the strong-coupling BEC regime of ^{40}K Fermi gas[1] seems difficult to explain as far as a simple uniform system is considered[16].

In this paper, we study pseudogap phenomena in a trapped Fermi gas above T_c , addressing the recent photoemission experiment by JILA group[1]. Extending our previous paper for a uniform Fermi gas to include effects of a harmonic trap within the local density approximation (LDA), we calculate the local DOS, as well as the local spectral weight (SW), over the entire BCS-BEC crossover region within the T -matrix approximation in terms of pairing fluctuations[16–20]. We clarify how the inhomogeneous pseudogap phenomenon appears in these quantities.

Recently, Refs. [21, 22] have studied the photoemission spectra using phenomenological theories with the BCS ansatz. While they capture some features of experimental results in the unitarity limit, they cannot explain the observed spectrum in the BEC regime, which consists of upper sharp and lower broad peaks. In contrast, including the inhomogeneous strong-coupling effect, we show that our *ab initio* calculation of the photoemission spectra can naturally explain the experiments[1] from the weak-coupling BCS to the strong-coupling BEC regimes, without introducing any free parameters.

We consider a two-component Fermi gas in a harmonic trap. Assuming a broad Feshbach resonance, we employ the ordinary BCS model, described by the Hamiltonian,

$$H = \sum_{\mathbf{p}, \sigma} \xi_{\mathbf{p}} c_{\mathbf{p}\sigma}^{\dagger} c_{\mathbf{p}\sigma} - U \sum_{\mathbf{q}, \mathbf{p}, \mathbf{p}'} c_{\mathbf{p}+\mathbf{q}/2\uparrow}^{\dagger} c_{-\mathbf{p}+\mathbf{q}/2\downarrow}^{\dagger} c_{\mathbf{p}'+\mathbf{q}/2\downarrow} c_{\mathbf{p}'+\mathbf{q}/2\uparrow}. \quad (1)$$

Here, $c_{\mathbf{p}\sigma}$ is the annihilation operator of a Fermi atom with pseudospin $\sigma = \uparrow, \downarrow$, and the kinetic energy $\xi_{\mathbf{p}} = \varepsilon_{\mathbf{p}} - \mu$ is measured from the chemical potential μ , where $\varepsilon_{\mathbf{p}} = p^2/2m$ and m is the atomic mass. The pairing interaction $-U (< 0)$ is assumed to be tunable by a Feshbach resonance[23], which is related to the s -wave scattering length a_s as[24] $4\pi a_s/m = -U/[1 - U \sum_{\mathbf{p}} 1/(2\varepsilon_{\mathbf{p}})]$.

Within a LDA, effects of a trap are conveniently in-

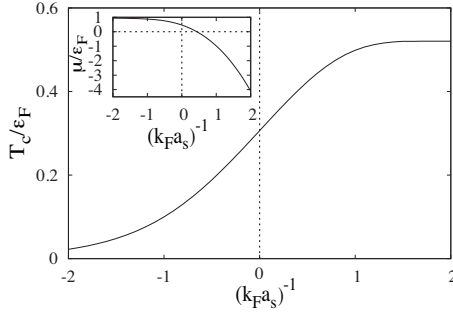


FIG. 1: Calculated T_c as a function of the inverse scattering a_s^{-1} . The inset shows μ at T_c . k_F is the Fermi momentum, and ϵ_F is the Fermi energy. We use these T_c and μ in Figs. 2-5.

incorporated into the theory by replacing the chemical potential μ by $\mu(r) \equiv \mu - V(r)$ [25], where $V(r) = m\omega_{tr}^2 r^2/2$ is a harmonic potential (where ω_{tr} is a trap frequency). The LDA single-particle Green's function is given by $G_{\mathbf{p}}(i\omega_n, r) = 1/[i\omega_n - \xi_{\mathbf{p}}(r) - \Sigma_{\mathbf{p}}(i\omega_n, r)]$, where $\xi_{\mathbf{p}}(r) = \epsilon_{\mathbf{p}} - \mu(r)$, and ω_n is the fermion Matsubara frequency. The LDA self-energy $\Sigma_{\mathbf{p}}(i\omega_n, r)$ involves effects of pairing fluctuations within the T -matrix approximation[16–20], which is given by $\Sigma_{\mathbf{p}}(i\omega_n, r) = T \sum_{\mathbf{q}, i\nu_n} \Gamma_{\mathbf{q}}(i\nu_n, r) G_{\mathbf{q}-\mathbf{p}}^0(i\nu_n - i\omega_n, r)$. Here, ν_n is the boson Matsubara frequency, and $G_{\mathbf{p}}^0(i\omega_n, r) = 1/[i\omega_n - \xi_{\mathbf{p}}(r)]$ is the LDA free fermion propagator. $\Gamma_{\mathbf{q}}(i\nu_n, r) = -U/[1 - U\Pi_{\mathbf{q}}(i\nu_n, r)]$ is the particle-particle scattering matrix within the T -matrix approximation, where $\Pi_{\mathbf{q}}(i\nu_n, r) = T \sum_{\mathbf{p}, i\omega_n} G_{\mathbf{p}+\mathbf{q}/2}^0(i\nu_n + i\omega_n, r) G_{-\mathbf{p}+\mathbf{q}/2}^0(-i\omega_n, r)$ is the pair propagator[10].

In this paper, we focus on the case at T_c to compare with the experiments in Ref. [1]. The region above T_c will be discussed elsewhere. In LDA, the superfluid phase transition is determined by the Thouless criterion at the trap center[26], i.e., $\Gamma_{\mathbf{q}=0}(i\nu_n = 0, r = 0)^{-1} = 0$ [10]. Strong-coupling effects on μ are included by solving this T_c -equation together with the equation for the total number of Fermi atoms, $N = 2T \int dr \sum_{\mathbf{p}, i\omega_n} G_{\mathbf{p}}(i\omega_n, r) e^{i\omega_n \delta}$.

Figure 1 shows the calculated T_c and μ as functions of $(k_F a_s)^{-1}$, where k_F is the Fermi momentum defined from the Fermi energy $\epsilon_F = (3N)^{1/3} \omega_{tr} = k_F^2/(2m)$. In Fig. 1, T_c in a trapped gas is found to be higher than that in a uniform gas in terms of ϵ_F [26, 27]. Using them, we calculate the local SW $A(\mathbf{p}, \omega, r)$ and local DOS $\rho(\omega, r)$ from the analytic continued Green's function as, respectively,

$$A(\mathbf{p}, \omega, r) = -\frac{1}{\pi} \text{Im}[G_{\mathbf{p}}(i\omega_n \rightarrow \omega + i\delta, r)], \quad (2)$$

$$\rho(\omega, r) = \sum_{\mathbf{p}} A(\mathbf{p}, \omega, r). \quad (3)$$

The photoemission spectrum[1] can be calculated in the same way as the rf-tunneling current spectroscopy[26, 28, 29], where atoms in one of the two pseudospin states ($\equiv |\uparrow\rangle$) are uncoupled into an unoccupied state $|3\rangle$

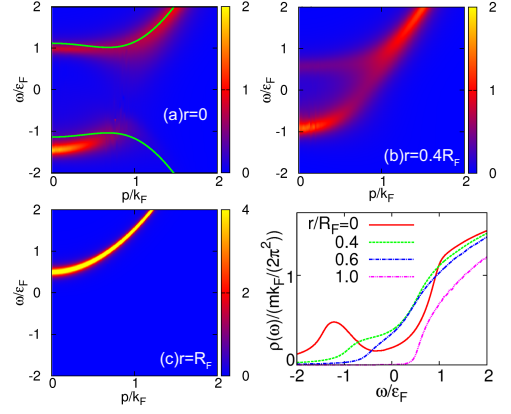


FIG. 2: (color online). (a)-(c) Intensity of local SW $A(\mathbf{p}, \omega, r)$ (units of ϵ_F^{-1}). (d) local DOS $\rho(\omega, r)$. We set $T = T_c$ and $(k_F a_s)^{-1} = 0$. The dotted line in (a) is the BCS-like quasiparticle spectrum with $\Delta_{pg} = 1.06$.

($\neq |\uparrow, \downarrow\rangle$) by an applied rf pulse. Since the final-state interaction can be safely neglected in ^{40}K Fermi gas[1, 21], the Hamiltonian for $|3\rangle$ is simply given by $H_3 = \sum_{\mathbf{p}} [\epsilon_{\mathbf{p}} + \omega_3 - \mu_3(r)] b_{\mathbf{p}}^\dagger b_{\mathbf{p}}$. Here, $b_{\mathbf{p}}$ describes the third pseudospin state $|3\rangle$, and ω_3 is the energy difference between $|\uparrow\rangle$ and $|3\rangle$. The chemical potential $\mu_3(r) = \mu_3 - V(r)$ involves trap effects within LDA. The transition from $|\uparrow\rangle$ to $|3\rangle$ is induced by the tunneling Hamiltonian[26, 28, 29] $H_T = t_F \sum_{\mathbf{k}} [e^{-i\omega_L t} b_{\mathbf{k}+\mathbf{q}_L}^\dagger c_{\mathbf{k}\uparrow} + \text{H.c.}]$, where t_F is a transfer matrix element, and \mathbf{q}_L and ω_L are the momentum and frequency of the rf-pulse, respectively. The photoemission spectrum is obtained from rf-tunneling current $I(\Omega, r)$ from $|\uparrow\rangle$ to $|3\rangle$, where $\Omega \equiv \omega_L - \omega_3$ is the rf-detuning. Within the linear response theory, we obtain $I(\Omega, r) = -i \int_{-\infty}^t dt' \langle [\hat{J}(r, t), H_T(r, t')] \rangle e^{\delta t'}$, where $J(t) \equiv -it_F \sum_{\mathbf{k}} e^{i(H+H_3)t} [e^{-i\omega_L t} b_{\mathbf{k}+\mathbf{q}_L}^\dagger c_{\mathbf{k}\uparrow} - \text{H.c.}] e^{-i(H+H_3)t}$ is the tunneling current operator in the Heisenberg representation, and $H_T(t) \equiv e^{i(H+H_3)t} H_T e^{-i(H+H_3)t}$. We thus obtain the rf-tunneling current $I(\Omega, r) = \sum_{\mathbf{p}} I(\mathbf{p}, \Omega, r)$, where the momentum-resolved photoemission spectrum $I(\mathbf{p}, \Omega, r)$ has the form

$$I(\mathbf{p}, \Omega, r) = 2\pi t_F^2 A(\mathbf{p}, \xi_{\mathbf{p}}(r) - \Omega, r) f(\xi_{\mathbf{p}}(r) - \Omega). \quad (4)$$

Here, $f(\Omega)$ is the Fermi distribution function. In Eq. (4), we have assumed that the momentum \mathbf{q}_L of rf-photon is negligible and $|3\rangle$ is initially empty ($f(\epsilon_p - \mu_3(r)) = 0$).

In a uniform Fermi gas, the photoemission spectrum is related to SW of occupied states as $I(\mathbf{p}, \Omega \rightarrow \xi_{\mathbf{p}} - \omega) = 2\pi t_F^2 A(\mathbf{p}, \omega) f(\omega)$. In particular, it is equal to SW below $\omega = 0$ at $T = 0$. When $T > 0$, thermally excited quasiparticles also contribute to the spectrum, so that $I(\mathbf{p}, \Omega \rightarrow \xi_{\mathbf{p}} - \omega)$ becomes finite even when $\omega > 0$.

In the photoemission experiment[1], since the rf-pulse is applied to the whole gas cloud, the observed spectrum involves contributions from all spatial regions of the cloud. To include this situation, we should take spatial

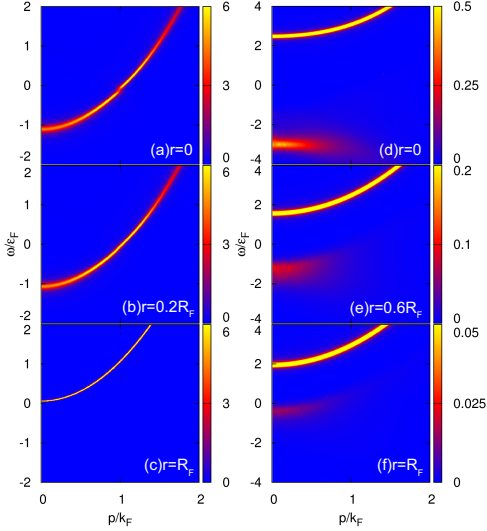


FIG. 3: (color online). Intensity of local SW $A(\mathbf{p}, \omega, r)$ (units of ε_F^{-1}). (a)-(c) $(k_F a_s)^{-1} = -1$. (d)-(f) $(k_F a_s)^{-1} = +1$. We set $T = T_c$.

average of Eq.(4) as

$$I_{\text{ave}}(\mathbf{p}, \Omega) = \frac{2\pi t_F^2}{V} \int dr A(\mathbf{p}, \xi_{\mathbf{p}}(r) - \Omega, r) f(\xi_{\mathbf{p}}(r) - \Omega). \quad (5)$$

Here, $V = 4\pi R_F^3/3$, where $R_F = \sqrt{2\mu/(m\omega_{\text{tr}}^2)}$ is the Thomas-Fermi radius[30]. We emphasize that this gives a proper definition for spatially averaged photoemission spectrum. For later convenience, we define the averaged occupied SW and DOS by, respectively,

$$\overline{A(\mathbf{p}, \omega) f(\omega)} \equiv I_{\text{ave}}(\mathbf{p}, \Omega \rightarrow \xi_{\mathbf{p}} - \omega)/(2\pi t_F^2), \quad (6)$$

$$\overline{\rho(\omega) f(\omega)} \equiv \sum_{\mathbf{p}} I_{\text{ave}}(\mathbf{p}, \Omega \rightarrow \xi_{\mathbf{p}} - \omega)/(2\pi t_F^2). \quad (7)$$

To see the basic characters of Eqs. (6) and (7), it is helpful to consider a free Fermi gas at $T = 0$. In this case, Eqs. (6) and (7) reduce to, respectively,

$$\overline{A(\mathbf{p}, \omega) f(\omega)} = |\omega/\mu|^{3/2} \delta(\omega - \xi_{\mathbf{p}}) \theta(-\omega), \quad (8)$$

$$\overline{\rho(\omega) f(\omega)} = (m^{3/2}/\sqrt{2\pi^2}) |\omega/\mu|^{3/2} \sqrt{\omega + \mu} \theta(\omega + \mu) \theta(-\omega). \quad (9)$$

In the former, the peak position gives the one-particle energy $\xi_{\mathbf{p}}$. In the latter, DOS in a uniform gas ($\propto \sqrt{\omega + \mu}$) is modified by the factor $|\omega|^{3/2}$.

We now show our numerical results. Figure 2 shows the local SW $A(\mathbf{p}, \omega, r)$ and DOS $\rho(\omega, r)$ at T_c in the unitarity limit ($(k_F a_s)^{-1} = 0$). In the trap center (panel (a)), a clear pseudogap structure exists, i.e., two prominent peaks appear along the particle branch and hole branch of the BCS-like quasiparticle spectrum $\omega = \pm \sqrt{\xi_{\mathbf{p}}^2 + \Delta_{\text{pg}}^2}$,

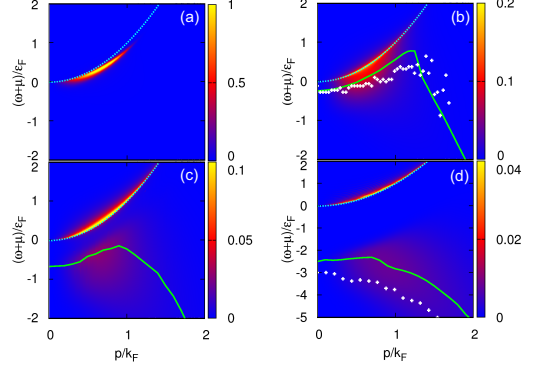


FIG. 4: (color online). Intensity of averaged occupied SW $p^2 A(\mathbf{p}, \omega) f(\omega)$ (units of $1/2m$) at T_c . The values of pairing interaction $(k_F a_s)^{-1}$ are (a) -1, (b) 0, (c) 0.4, and (d) 1. The dashed line indicates the spectrum of a free Fermi gas $\xi_{\mathbf{p}}$. The solid line is the lower peak position of intensity. Symbols are corresponding experimental data [1].

where the superfluid gap Δ is replaced by the pseudogap Δ_{pg} . The origin of Δ_{pg} is a particle-hole coupling by pairing fluctuations[16–20]. Since pairing fluctuations also induce a finite lifetime of quasiparticle excitations, the particle and hole branches in Fig. 2(a) have finite widths, which is in contrast to the mean-field BCS case, where both branches appear as δ -functional peaks. We note that the deviation of the lower peak from the BCS-like quasiparticle spectrum is considered due to the presence of excited pairs [16, 20].

Pairing fluctuations are weak around the edge of the gas due to low particle density. Thus, the pseudogap in the local SW gradually disappears, as one leaves from the trap center. (See Figs. 2(b) and (c).) In panel (c), a single sharp peak line only exists near the one-particle energy of a free Fermi gas $\xi_{\mathbf{p}}(R_F)$. Namely, the gas is pseudogapped in the center of the trap, while it is nearly non-interacting on its edges.

These inhomogeneous features can be also seen in local DOS. As shown in Fig. 2(d), while a large dip structure (which is a characteristic pseudogap effect in DOS) appears around $\omega = 0$ in the trap center, local DOS is almost equal to that of a free Fermi gas ($\rho(\omega, r) = (m^{3/2}/(\sqrt{2\pi^2})) \sqrt{\omega + \mu(r)}$) when $r = R_F$. Since spatial inhomogeneity is unique to trapped Fermi gases, the observation of local SW and DOS by using the tomographic techniques[31, 32] would be interesting.

We note that the inhomogeneous pseudogap structure depends on the strength of pairing interaction. When pairing fluctuations are weak in the BCS regime, the double-peak structure in $A(\mathbf{p}, \omega, r)$ soon disappears, as one leaves from the trap center. (See Figs. 3(a)-(c).) In contrast, Figs. 3(d)-(f) show that the pseudogap features persist even near the edge of the gas in the BEC regime.

Figures 4 and 5, respectively, show the averaged occupied SW and DOS at T_c . In the weak-coupling BCS regime, these quantities are expected to be close to the

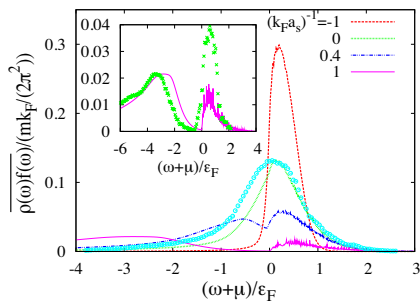


FIG. 5: (color online). Averaged occupied DOS $\overline{\rho(\omega)f(\omega)}$ at T_c . The inset shows a magnification of the curve for $(k_F a_s)^{-1} = 1$. Circles and crosses show the experimental data for $(k_F a_s)^{-1} = 0$ and 1, respectively[1]. The data are fitted so that the peak value coincides with that of theory curves. The data agree well with the theory curves.

free Fermi gas results in Eqs. (8) and (9). Indeed, the position of the peak line in Fig. 4(a) is almost at the single-particle energy of a free fermion $\omega = \xi_{\mathbf{p}} (\leq 0)$, and the averaged occupied DOS in Fig. 5 is close to DOS for a free Fermi gas multiplied by $|\omega|^{3/2}$ when $(k_F a_s)^{-1} = -1$. However, we also find that the peak line in Fig. 4(a) is slightly below the curve of $\omega = \xi_{\mathbf{p}}$, which is a signature of pseudogap effect near the trap center. Namely, the pseudogap Δ_{pg} lowers the hole branch as $-|\xi_{\mathbf{p}}(r)| \rightarrow -\sqrt{\xi_{\mathbf{p}}^2(r) + \Delta_{\text{pg}}^2}$, and this effect still remains even after spatial average.

In the crossover region, pairing fluctuations are strong around the trap center. In the unitarity limit, while the region around the edge of the gas still gives a sharp peak line at $\omega \simeq \xi_{\mathbf{p}}$ in $A(\mathbf{p}, \omega)f(\omega)$, the pseudogap in SW around $r = 0$ causes the broadening of the lower part of the peak line around $p/k_F \simeq 0.5$ shown in Fig. 4(b). In addition, short lifetime of quasiparticle excitations by strong pairing fluctuations around the trap center also causes the broadening of $\overline{\rho(\omega)f(\omega)}$, as shown in Fig. 5.

We also note that one can see the back-bending of the lower peak position in Figs. 4(b)-(d) originating from the lower branch shown in Fig. 2(a), which well agrees with the experimental data[1].

In the BEC regime, the pseudogap features persist to the edge of the gas. Thus, the double-peak structure in the local SW (See Figs. 3(d)~(f).) is not smeared out by spatial average, as shown in Figs. 4(c)~(d). In particular, the double-peak structure in panel (d), consisting of upper *sharp* peak and lower *broad* peak, agrees well with the photoemission experiment by JILA group[1]. We emphasize that this spectral structure cannot be explained within the previous phenomenological theories[21, 22]. Such a double-peak structure also appears in Fig. 5, which is also consistent with the experiment[1].

In the BEC limit, the spectral weight only has the upper sharp peak describing the dissociation of two-body bound molecules. On the other hand, as discussed in Ref. [16], the lower broad peak in SW in the BEC regime is an evidence of many-body character of paired atoms. Thus, the double-peak structure in Figs. 4(c)~(d) may be understood as a result of the fact that, in the BCS-BEC crossover, the character of fermion pair continuously changes from the many-body bound state associated with the Cooper instability to the two-body bound state where the Fermi surface is not necessary.

To summarize, we have discussed inhomogeneous pseudogap effect in the BCS-BEC crossover regime of a trapped Fermi gas. Including this effect, we showed that calculated spatially averaged photoemission spectrum agrees well with the recent experiment by JILA group[1]. Since spatial inhomogeneity by a trap is inevitable in a cold Fermi gas, our results would be useful for clarifying strong-coupling phenomena of this system over the entire BCS-BEC crossover region.

We wish to thank A. Griffin for useful discussions. We acknowledge J. P. Gaebler and D. S. Jin for providing us with their experimental data.

-
- [1] J. T. Stewart *et al.*, Nature **454**, 744 (2008).
[2] A. Damascelli *et al.*, Rev. Mod. Phys. **75**, 473 (2003).
[3] For reviews, see Q. J. Chen *et al.*, Phys. Rep. **412**, 1 (2005); I. Bloch *et al.*, Rev. Mod. Phys. **80**, 885 (2008); S. Giorgini *et al.*, Rev. Mod. Phys. **80**, 1215 (2008).
[4] C. A. Regal *et al.*, Phys. Rev. Lett. **92**, 040403 (2004).
[5] M. Zwierlein *et al.*, Phys. Rev. Lett. **92**, 120403 (2004).
[6] J. Kinast *et al.*, Phys. Rev. Lett. **92**, 150402 (2004).
[7] M. Bartenstein *et al.*, Phys. Rev. Lett. **92**, 203201 (2004).
[8] D. M. Eagles, Phys. Rev. **186**, 456 (1969).
[9] A. J. Leggett, in *Modern Trends in the Theory of Condensed Matter* ed. by Pekalski and Przystawa (Springer, Berlin, 1980) p.14.
[10] P. Nozières and S. Schmitt-Rink, J. Low Temp. Phys. **59**, 195 (1985).
[11] C. Sá de Melo *et al.*, Phys. Rev. Lett. **71**, 3202 (1993).
[12] E. Timmermans *et al.*, Phys. Lett. A **285**, 228 (2001).
[13] M. Holland *et al.*, Phys. Rev. Lett. **87**, 120406 (2001).
[14] Y. Ohashi *et al.*, Phys. Rev. Lett. **89**, 130402 (2002).
[15] P. Lee *et al.*, Rev. Mod. Phys. **78**, 17 (2006).
[16] S. Tsuchiya *et al.*, Phys. Rev. A **80**, 033613 (2009).
[17] B. Jankó *et al.*, Phys. Rev. B **56**, R11407 (1997).
[18] D. Rohe *et al.*, Phys. Rev. B **63**, 224509 (2001).
[19] Y. Yanase *et al.*, J. Phys. Soc. Jpn. **70**, 1659 (2001).
[20] A. Perali *et al.*, Phys. Rev. B **66**, 024510 (2002).
[21] Q. Chen *et al.*, Phys. Rev. Lett. **102**, 190402 (2009).
[22] T.-L. Dao *et al.*, Phys. Rev. A **80**, 023627 (2009).
[23] For a review, see C. Chin *et al.*, arXiv:0812.1496.
[24] M. Randeria, in *Bose-Einstein Condensation*, ed. by A. Griffin, D. W. Snoke, and S. Stringari (Cambridge University Press, New York, 1995), p. 355.
[25] C. Pethick and H. Smith, *Bose-Einstein Condensation in Dilute Gases* (Cambridge University Press, Cambridge, United Kingdom, 2002).

- [26] Y. Ohashi *et al.*, Phys. Rev. A **72**, 013601 (2005).
- [27] A. Perali *et al.*, Phys. Rev. Lett. **92**, 220404 (2004).
- [28] P. Törma and P. Zoller, Phys. Rev. Lett. **85**, 487 (2000).
- [29] Y. He *et al.*, Phys. Rev. A **72**, 011602(R) (2005).
- [30] The spatial integration is taken up to $1.5R_F$, so that the occupied DOS converges.
- [31] Y. Shin *et al.*, Phys. Rev. Lett. **99**, 090403 (2007).
- [32] A. Schirotzek *et al.*, Phys. Rev. Lett. **101**, 140403 (2008).